Robust Global Observer Position-Yaw Control based on Ellipsoid Method for Quadrotors

Fatima Oliva-Palomo, Anand Sanchez-Orta, H Alazkio, Pedro Castillo Garcia, Aldo-Jonathan Muñoz-Vázquez

Robust Global Observer Position-Yaw Control based on Ellipsoid Method for Quadrotors

Fátima Oliva-Palomo[a,1], Anand Sanchez-Orta[a,1],
Hussain Alazki[b,2], Pedro Castillo[c,3], Aldo-Jonathan Muñoz-Vázquez[d,4]

[a] *Robotics and Advanced Manufacturing Division, Research Center for Advanced Studies (CINVESTAV), Saltillo México.*
[b] *Department of Mechatronics, Autonomous University of Carmen (UNACAR), Mexico.*
[c] *Sorbonne Universités, Université de Technologie de Compiègne, CNRS UMR 7253 Heudiasyc Lab., CS 60319,60203 Compiègne France.*
[d] *Texas A&M University, Division of Engineering, College Station Texas, USA.*

Abstract

An observed-based control strategy for position-yaw tracking of quadrotors is proposed. From a virtual controller for the position dynamics, attitude and angular velocity references are estimated with the aim of allowing the position-control components to enforce the tracking of a position reference. In addition, no measurement of the linear velocity is assumed, and the measurement of the position signal is noisy, thus, a dynamic observer for the position dynamics is employed. The ellipsoid method is considered to estimate the feedback controller and observer gains, based on an optimization procedure, in order to produce the ultimately boundedness of attitude and position tracking errors inside a compact convex vicinity of the origin, whose Lebesgue measure is minimized via LMIs. The advantages of the proposed scheme are illustrated through numerical simulations that include aerodynamic disturbances and noisy measurements. Finally, an experimental assessment is carried out to illustrate the feasibility and performance of the proposed controller in a real-time application.

Keywords: Position Control, Unmanned Aerial Vehicle, Real-time Validation, Quaternion Control.

1. Introduction

The quadrotor is a highly maneuverable vehicle that is capable of performing aggressive trajectories. This characteristics make it attractive for many different applications. Unfortunately, the fast dynamics and disturbances make it prone to oscillations, therefore, this small vehicle requires a fast and robust controller. The controller of the full actuated attitude dynamics has to guarantee the stability of the entire system, whilst being fast enough, considering that the position dynamics depend on the attitude [1, 2]. For this purpose, several contributions have been reported, some of them using the Euler angles as attitude representation because are more intuitive, but such representation has singularities [3, 4, 5, 6, 7, 8, 9, 10, 11], which can restrict the attitude space [4], discarding the tracking of highly aggressive maneuvers. Additionally, the use of quaternion algebra has been employed for using Euler parameters for attitude representation, avoiding singularities to produce a global controller [12], even for aggressive maneuvers [13, 14, 15]. Taking in to account aerodynamic disturbances, there some control approaches consider sliding mode [9, 16, 17] or adaptive [18] controllers, which can induce high frequencies in the controller signals, increasing the oscillation of the system. Recently, a neuroadaptive integral robust controller for visual quadrotor tracking is proposed in [19]. Asymptotic stability of the closed-loop system is guaranteed using Barbalat's lemma, however, conservative bounds of uncertainties are assumed to compute the controller gains and only simulations are provided.

Additionally, given the underactuation of the vehicle, the attitude has to be slaved to the position to allow tracking. How to modify the attitude dynamics makes the position control a nontrivial problem, for which, different strategies have been developed to solve underactuation. One approach is based on a position controller that is accounted for a disturbance to the attitude dynamics [20], which causes the vehicle to tilt to the desired direction in order to track the position reference, however, it has the drawback that the attitude controller is capable to compensate at least a part of the position controller, leading to a large position error. Another method consists in computing the desired attitude reference from the desired position trajectory [6], but in that case, all dynamic parameters have to be known in order to compute an accurate trajectory for the attitude dynamics, and even so, any of the disturbance causes a poor performance. A further more strategy is to compute the desired attitude from the desired acceleration that can be in turns computed from a

[1] (fatima.oliva, anand.sanchez)@cinvestav.mx
[2] halazki@pampano.unacar.mx
[3] castillo@hds.utc.fr
[4] aldo.munoz-vazquez@tamu.edu

virtual controller [18], nevertheless, in this method the rotation about the z axis is restrained at 0 in order to allow the tracking, leavening one degree of freedom unused. In addition, a virtual controller (desired force on the vehicle) can be used in order to compute the desired references for the attitude [5], leaving only the design of a controller that does not induce high frequencies in the system dynamics.

By virtue of the aforementioned discussion, it is evident that the quadrotor needs a robust controller to compensate for dynamic disturbances, whilst avoiding high frequencies and kinematic singularities. Along this direction, the attractive ellipsoid method allows one to design a continuous controller that is robust against a broad class of disturbances and uncertainties, assuring practical stability [21]. It is assumed that there is not complete information of the plant, such as the external disturbances, but at least, an upper bound is known. In this methodology, the feedback gains are calculated from an optimization problem, where Linear Matrix inequalities (LMIs) appear, and by solving them numerically, the region at which the tracking errors converge is reduced. The solution of convex inequalities has allowed the development of important contributions to the control of aerial vehicles, such as the computation of observer gains in fault estimation schemes [22].

The contribution is then, an observer based on position feedback by using the Ellipsoid Method. The virtual controller is defined in the position dynamics, which represents the desired force in the vehicle for position tracking. From the virtual controller, the attitude references are estimated, which are represented by unit quaternions in order to avoid possible singularities. Additionally, a desired rotation about the z axis is performed while tracking the position. The controller is designed based on the ellipsoid method, assuring a small region at which the errors converge, depending on the solution of LMIs to estimate the optimal gains. The validity of proposed scheme is shown throughout a simulation study, subject to a time-varying wind gust and noisy measurements, and experimental results, which confirm the robustness of the proposed controller to wide range of uncertainties and disturbances.

2. Background and Problem statement

2.1. Quadrotor Dynamic Model

Let $\mathcal{I} = \{e_x, e_y, e_z\}$ be the earth fixed frame, and $\mathcal{B} = \{e_x^b, e_y^b, e_z^b\}$ the body fixed frame, whose origin coincides with the center of mass, see Fig. 1. The orientation of the rigid body is given by an orthogonal rotation matrix $R \in \mathsf{SO}(3) : \mathcal{I} \to \mathcal{B}$. The Newton-Euler equations of motion representing the position and orientation dynamics of the quadrotor are

$$m\ddot{\xi} = -TR(\overline{q})e_z + mge_z + f_d(t) \quad (1)$$

$$\dot{\overline{q}} = \frac{1}{2}\overline{q} \otimes \overline{\Omega} \quad (2)$$

$$J\dot{\Omega} = -\Omega \times J\Omega + \tau + \tau_d(t) \quad (3)$$

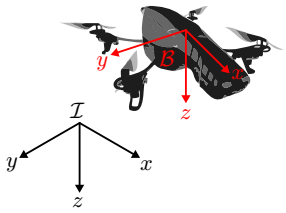

Figure 1: Inertial and body frames in the vehicle.

where $\xi = [\xi_x, \xi_y, \xi_z]^\mathsf{T} \in \mathcal{I}$ is the position of the vehicle, $e_z = [0, 0, 1]^\mathsf{T}$, $m \in \mathbb{R}$ is the mass, $g \in \mathbb{R}$ represents the gravitational acceleration magnitude, $f_d(t) \in \mathcal{I}$ denotes the bounded disturbance forces, $\overline{q} = [q_0, q_1, q_2, q_3]^\mathsf{T} \in \mathcal{S}^3$ is the unit quaternion that represents the rotation of the vehicle, whose scalar and vector parts are $q_0 \in \mathbb{R}$ and $q = [q_1, q_2, q_3]^\mathsf{T}$, respectively, this leads to

$$\overline{q} = \begin{bmatrix} q_0 \\ q \end{bmatrix} = \begin{bmatrix} \cos(\theta) \\ \lambda \sin(\theta). \end{bmatrix} \quad (4)$$

The quaternion product $\otimes$ is given by [23]

$$\overline{p} \otimes \overline{q} = \begin{bmatrix} p_0 & -p^\mathsf{T} \\ p & I_{3\times 3}p_0 + [p\times] \end{bmatrix} \begin{bmatrix} q_0 \\ q \end{bmatrix} \quad (5)$$

and the conjugate of a quaternion is

$$\overline{q}^* = [q_0, -q_1, -q_2, -q_3]^\mathsf{T} \quad (6)$$

Note that, in the case unit quaternions, $\overline{q}^* = \overline{q}^{-1}$. $\overline{\Omega} = [0, \Omega^\mathsf{T}]^\mathsf{T}$ denotes a pure quaternion with scalar part of zero and vector part Ω, where $\Omega = [\Omega_1, \Omega_2, \Omega_3]^\mathsf{T} \in \mathcal{B}$ defines the angular velocity of the airframe. In addition the rotation matrix $R(\overline{q})$ is expresed in terms of the unit quaternion, as is equivalent to

$$\overline{v}_i = \overline{q} \otimes \overline{v}_b \otimes \overline{q}^* = \begin{bmatrix} 0 \\ R(\overline{q})v_b \end{bmatrix}, \quad (7)$$

where $\overline{v}_i$ and $\overline{v}_b$ are pure quaternions, $v_i = [v_{i1}, v_{i2}, v_{i3}]^\mathsf{T} \in \mathcal{I}$, $v_b = [v_{b1}, v_{b2}, v_{b3}]^\mathsf{T} \in \mathcal{B}$, and $R(\overline{q})$ is given by

$$R(\overline{q}) = \begin{bmatrix} 1 - 2q_2^2 - 2q_3^2 & 2q_1q_2 - 2q_0q_3 & 2q_1q_3 + 2q_0q_2 \\ 2q_1q_2 + 2q_0q_3 & 1 - 2q_1^2 - 2q_3^2 & 2q_2q_3 - 2q_0q_1 \\ 2q_1q_3 - 2q_0q_2 & 2q_2q_3 + 2q_0q_1 & 1 - 2q_1^2 - 2q_2^2 \end{bmatrix} \quad (8)$$

$J \in \mathbb{R}^{3\times 3}$ stands for the constant inertia matrix around the center of mass and is expressed in the body fixed frame $\mathcal{B}$. The matrix $[\Omega\times] \in \mathbb{R}^{3\times 3}$ denotes the skew-symmetric matrix of the vector Ω

$$[\Omega\times] = \begin{bmatrix} 0 & -\Omega_3 & \Omega_2 \\ \Omega_3 & 0 & -\Omega_1 \\ -\Omega_2 & \Omega_1 & 0 \end{bmatrix}, \quad (9)$$

the external bounded torque disturbance is $\tau_d(t)$, and $\tau \in \mathcal{B}$ is the control torque.

2.2. The Class of quasi-Lipschitz Functions

The quadrotor model is nonlinear, then the following definition will be useful in the stability analysis.

Definition 1[24]: A vector function $g : \mathbb{R}^n \to \mathbb{R}^k$ is said to be from the class $\mathcal{C}(C, \delta_0, \delta_1)$ of *quasi-Lipschitz* functions if there exists a matrix $C \in \mathbb{R}^{k\times n}$ and nonnegative constants δ_0 and δ_1 such that for any $x \in \mathbb{R}^n$ the following inequality holds:

$$\|g(x) - Cx\|^2 \leq \delta_0 + \delta_1\|x\|^2 \tag{10}$$

This implies that the growth rates of $g(x)$ as $\|x\| \to \infty$ are not faster than linear, [21]. Notice that if $C = 0$, $\delta_0 = 0$ and $g(0) = 0$ the inequality (10) characterizes the Lipschitz continuity property of the function $g(x)$ with the Lipschitz constant $L = \sqrt{\delta_1}$.

2.3. Attractive Ellipsoids

In order to determine the convergence region and to apply the ellipsoid method, the following definition is needed.

Definition 2 [21]: An ellipsoid, represented by $\varepsilon \subset \mathbb{R}^n$ with center in x_c is given by:

$$\varepsilon = \left\{x \in \mathbb{R}^n |\ \ (x - x_c)^\mathsf{T} P(x - x_c) \leq 1\right\} \tag{11}$$

is said to be **attractive** for the trajectories x :

$$\limsup_{t\to\infty} (x - x_c)^\mathsf{T} P(x - x_c) \leq 1$$

where the ellipsoidal matrix P is a symmetric positive definite matrix $0 < P = P^\mathsf{T} \in \mathbb{R}^{n\times n}$,

2.4. Problem formulation

The problem is to design a closed-loop controller allowing robust position tracking for system (3), assuring that the error trajectories are confined to an invariant attractive set. The controller is continuous and independent of model parameters, but its design consider the system model, ensuring robustness to parametric uncertainties, aerodynamical effects and exogenous disturbances. In addition, considering underactuation, the desired attitude consigns that guarantee position tracking are also needed.

3. Mapping based Position Control for a Quadrotor

The quadrotor is an underactuated vehicle, then, in order to reach a desired position, the vehicle needs to rotate to change the direction of the thrust to generate force components in a desired direction. In consequence, the vehicle gives up some degrees of freedom in the attitude to gain degrees of freedom in position. In this sense, a virtual control u_d is defined, where the components of this vector corresponds to the input forces needed to track the desired position. Then, the virtual controller u_d corresponds to the desired thrust T_d in a desired direction, which is defined by rotation represented by the unit quaternion q_d,

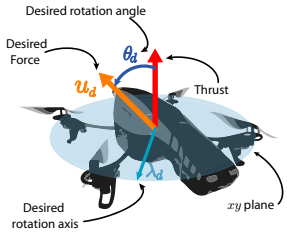

Figure 2: The attitude is "sacrificed" in order to control the position.

see Fig. 2, consequently the virtual control can be defined as

$$u_d = -T_d R(\bar{q}_d) e_z \tag{12}$$

Therefore, using (4), (8), (12), and considering that the magnitude of the virtual controller is the desired thrust T_d, then the vector that define the desired direction $\hat{u}_d = \frac{u_d}{\|u_d\|} = -R(\bar{q}_d)e_z$ and is given by

$$\hat{u}_d = \begin{bmatrix} -2q_{1d}q_{3d} - 2q_{0d}q_{2d} \\ -2q_{2d}q_{3d} + 2q_{0d}q_{1d} \\ -1 + 2q_{1d}^2 + 2q_{2d}^2 \end{bmatrix} = \begin{bmatrix} \hat{u}_{d_1} \\ \hat{u}_{d_2} \\ \hat{u}_{d_3} \end{bmatrix} \tag{13}$$

Now using the unit quaternion restriction $q_{0d}^2 + q_{1d}^2 + q_{2d}^2 + q_{3d}^2 = 1$ and from (13), the scalar part of the quaternion, expressed in terms of q_{3d} and $\hat{u}_{d_3}$, equals to

$$q_{0d} = \frac{1}{2}\sqrt{-2\hat{u}_{d_3} + 2 - 4q_{3d}^2} \tag{14}$$

then, from (13) and (14), the solution for q_{1d} and q_{2d} is given by

$$\begin{aligned} \begin{bmatrix} q_{1d} \\ q_{2d} \end{bmatrix} &= \frac{1}{2(q_{0d}^2 + q_{3d}^2)} \begin{bmatrix} -q_{3d} & q_{0d} \\ -q_{0d} & -q_{3d} \end{bmatrix} \begin{bmatrix} \hat{u}_{d_1} \\ \hat{u}_{d_2} \end{bmatrix} \\ &= \begin{bmatrix} \frac{q_{3d}}{\hat{u}_{d_3} - 1} & -\frac{1}{2}\frac{\sqrt{-2\,\hat{u}_{d_3} + 2 - 4\,q_{3d}^2}}{\hat{u}_{d_3} - 1} \\ \frac{1}{2}\frac{\sqrt{-2\,\hat{u}_{d_3} + 2 - 4\,q_{3d}^2}}{\hat{u}_{d_3} - 1} & \frac{q_{3d}}{\hat{u}_{d_3} - 1} \end{bmatrix} \begin{bmatrix} \hat{u}_{d_1} \\ \hat{u}_{d_2} \end{bmatrix} \end{aligned} \tag{15}$$

The scalar part q_{0d} and the two components of the vector part q_{1d} and q_{2d} are in terms of q_{3d} and the direction defined by the vector $\hat{u}_d$. Given that there is no restriction of which value should be q_{3d}, let define the final rotation in two steps. First, assuming that the desired rotation axis is in the xy plane, ie $q_{3d} = 0$, the desired quaternion equals to

$$\bar{q}_{d_{xy}} = \begin{bmatrix} \frac{1}{2}\sqrt{-2\hat{u}_{d_3} + 2} \\ \frac{\hat{u}_{d_2}}{\sqrt{-2\hat{u}_{d_3} + 2}} \\ \frac{-\hat{u}_{d_1}}{\sqrt{-2\hat{u}_{d_3} + 2}} \\ 0 \end{bmatrix} \tag{16}$$

After the vehicle is rotated to generate the desired force components, we can perform another rotation of a desired ψ_d angle about the z axis on the body of the quadrotor,

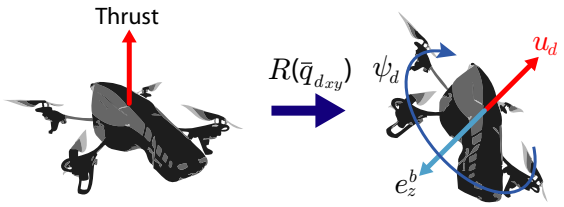

Figure 3: The final rotation about the z axis does not change the direction of the original desired force.

as can be seen in Fig. 3, this rotation is defined by

$$\bar{q}_{d_z} = \begin{bmatrix} \cos\left(\frac{\psi_d}{2}\right) \\ 0 \\ 0 \\ \sin\left(\frac{\psi_d}{2}\right) \end{bmatrix}, \tag{17}$$

This last rotation does not change the direction of the desired force, which implies that the tracking of the position it is not modified. Therefore, the desired quaternion for the attitude is given by the consecutive rotations of $\bar{q}_{d_{xy}}$ and $\bar{q}_{d_z}$ as follows

$$\bar{q}_d = \bar{q}_{d_{xy}} \otimes \bar{q}_{d_z} = \begin{bmatrix} \frac{1}{2}\sqrt{-2\hat{u}_{d_3}+2}\cos\left(\frac{\psi_d}{2}\right) \\ \frac{-\hat{u}_{d_1}\sin\left(\frac{\psi_d}{2}\right)+\hat{u}_{d_2}\cos\left(\frac{\psi_d}{2}\right)}{\sqrt{-2\hat{u}_{d_3}+2}} \\ \frac{-\hat{u}_{d_1}\cos\left(\frac{\psi_d}{2}\right)-\hat{u}_{d_2}\sin\left(\frac{\psi_d}{2}\right)}{\sqrt{-2\hat{u}_{d_3}+2}} \\ \frac{1}{2}\sqrt{-2\hat{u}_{d_3}+2}\sin\left(\frac{\psi_d}{2}\right) \end{bmatrix} \tag{18}$$

Note that in (15) q_{1d} and q_{2d} are not well defined if $\hat{u}_{d_3} = 1$, that means that the direction of the desired force is e_z. It is assumed that this scenario is highly improbable due to the gravitational force compensation in the control law, which means that the component $\hat{u}_{d_3}$ is always pointing upwards or $\hat{u}_{d_3} < 0$. Also, note that the desired quaternion in (18) is equivalent to the equations (14) and (15) using $q_{3d} = \frac{1}{2}\sqrt{-2\hat{u}_{d_3}+2}\sin\left(\frac{\psi_d}{2}\right)$.

Now, to obtain the desired angular velocity, from (2), there exists a correspondence between the desired quaternion and the desired angular velocity, and its given by

$$\dot{\bar{q}}_d = \frac{1}{2}\bar{q}_d \otimes \bar{\Omega}_d \tag{19}$$

then, the desired angular velocity is equal to

$$\bar{\Omega}_d = 2\,\bar{q}_d^* \otimes \dot{\bar{q}}_d \tag{20}$$

with the time derivative of (18), $\hat{u}_d^{\mathsf{T}}\hat{u}_d = 1$, its derivative $\hat{u}_d^{\mathsf{T}}\dot{\hat{u}}_d = 0$, we obtain that (20) is a pure quaternion and the angular velocity equals to

$$\Omega_d = \begin{bmatrix} -\sin(\psi_d)\dot{\hat{u}}_{d_1}+\cos(\psi_d)\dot{\hat{u}}_{d_2}+\frac{\dot{\hat{u}}_{d_3}\left(\sin(\psi_d)\hat{u}_{d_1}-\cos(\psi_d)\hat{u}_{d_2}\right)}{\hat{u}_{d_3}-1} \\ -\cos(\psi_d)\dot{\hat{u}}_{d_1}-\sin(\psi_d)\dot{\hat{u}}_{d_2}+\frac{\dot{\hat{u}}_{d_3}\left(\cos(\psi_d)\hat{u}_{d_1}+\sin(\psi_d)\hat{u}_{d_2}\right)}{\hat{u}_{d_3}-1} \\ \dot{\psi}_d+\frac{\hat{u}_{d_1}\dot{\hat{u}}_{d_2}-\hat{u}_{d_2}\dot{\hat{u}}_{d_1}}{\hat{u}_{d_3}-1} \end{bmatrix} \tag{21}$$

Note that for the computation of the desired angular velocity the time derivative of the virtual position control $\dot{u}_d$ is needed, therefore this controller needs to be at least one time differentiable.

4. Attitude Control Design

With the purpose of allow to generate the desired input forces defined by the virtual control, an attitude controller has to assure that the systems tracks the desired references computed from the virtual controller. The control has to compensate the disturbances and aerodynamical effects present in the attitude dynamics and the design has to consider the nonlinearities of the model.

In order to design the attitude controller, first let define the attitude and angular velocity errors.

4.1. Attitude Error Equations

The rotation error quaternion is defined by

$$\bar{q}_e \triangleq \bar{q}_d^* \otimes \bar{q} \tag{22}$$

which represent the rotation difference between the actual and the desired attitude. Now to obtain the relation of the quaternion error and a angular velocity error, we obtain the derivative of (22), using (2), (6), (5), (19) and (22), is equal to

$$\dot{\bar{q}}_e = \frac{1}{2}\bar{q}_e \otimes \bar{\Omega}_e \tag{23}$$

where the error of angular velocity is

$$\Omega_e = \Omega - R^{\mathsf{T}}(\bar{q}_e)\Omega_d \tag{24}$$

The attitude dynamics has 3 degrees of freedom, the same that the unit quaternion has (4 different parameters and one restriction $\|\bar{q}_e\| = 1$). Assuring the 3 components of the vector part $q_e \to 0$ implies that the scalar part $q_{0e} \to \pm 1$, then we only need to assure $q_e \to 0$ in order to have $\bar{q} \to \bar{q}_d$. Also, considering small errors, with $q_{0e} \approx 1$, it can be assumed that the scalar part of the quaternion error doesn't change sign, if the initial condition is $q_{0e}(t_0) \approx 1$ that means that $q_{e_0} \geq 0$ and with the unit quaternion restriction, then

$$q_{e_0} = \sqrt{1 - q_{e_1}^2 - q_{e_2}^2 - q_{e_3}^2} \tag{25}$$

with this the differential equation of the vectorial part of the quaternion is given by

$$\dot{q}_e = \tilde{Q}(q_e)\Omega_e,\ \tilde{Q}(q_e) = \frac{1}{2}\left[(1 - q_e^{\mathsf{T}}q_e)^{1/2}I_{3\times 3} + [q_e\times]\right] \tag{26}$$

Now the state space can be defined by error variables that must converge to a small invariant set as follows

$$x_a = \begin{bmatrix} q_e \\ \Omega_e \end{bmatrix}, \quad \dot{x}_a = B_a\tau + \zeta_a(x_a, \Omega, \Omega_d, \dot{\Omega}_d, t) \tag{27}$$

where $\zeta_a(x_a, \Omega_d, \dot{\Omega}_d, t)$ corresponds to the disturbances and non-linearities of the attitude dynamics

$$\zeta(x_a, \Omega_d, \dot{\Omega}_d, t) = \begin{bmatrix} \tilde{Q}(q_e)\Omega_e \\ J^{-1}(-\Omega \times J\Omega + \tau_d) - R_e^{\mathsf{T}}\dot{\Omega}_d - R_e^{\mathsf{T}}\Omega_d \times \Omega_e \end{bmatrix}$$

and $B_a = [0_{3\times3}\ J^{-1\mathsf{T}}]^{\mathsf{T}}$

From (27), the quasi-linear model can be represented as

$$\dot{x}_a = A_a x_a + B_a \tau + \varphi_a(x_a, \Omega_d, \dot{\Omega}_d, t) \tag{28}$$

where $\varphi(x_a, \Omega, \Omega_d, \dot{\Omega}_d, t) = \zeta(x_a, \Omega, \Omega_d, \dot{\Omega}_d, t) - A_a x_a$, $A_a = \begin{bmatrix} -aI_{3\times3} & \frac{1}{2}I_{3\times3} \\ 0_{3\times3} & 0_{3\times3} \end{bmatrix}$, with $a > 0 \in \mathbb{R}$ is a positive scalar. The form of A_a comes from the linearization around the origin of $\tilde{Q}(q)$ and the constant a for and additional parameter for the solution of the ellipsoid method.

4.2. Assumptions of the attitude dynamics

Assumption 1: The desired Ω_d and $\dot{\Omega}_d$ are defined by the user, and are bounded by

$$\|\Omega_d\|^2 \leq \Omega_d^+ \quad \|\dot{\Omega}_d\|^2 \leq \dot{\Omega}_d^+ \tag{29}$$

Assumption 2: The norm of the disturbances vector τ_d has an upper bound, then there exists a positive constant d^+ such that

$$\|\tau_d\|^2 < d^+ \tag{30}$$

Assumption 3: The nonlinear term in (3) can be bounded using two constants $c_0 \geq 0$ and $c_1 > 0$ such that

$$\|J^{-1}(-\Omega \times J\Omega)\|^2 \leq c_0 + c_1\|\Omega\|^2 \ \forall\ \Omega \in \mathbb{R}^3 \tag{31}$$

4.3. Bound of the nonlinearities and disturbances

Now with the purpose of proceed to the stability analysis, the bound of φ is needed. With the assumptions 1-3, the norm of $\varphi(x, \Omega_d, \dot{\Omega}_d, t)$ is calculated as

$$\varphi(x_a, \Omega_d, \dot{\Omega}_d, t)^{\mathsf{T}}\varphi(x, \Omega_d, \dot{\Omega}_d, t) = \varphi_1^{\mathsf{T}}\varphi_1 + \varphi_2^{\mathsf{T}}\varphi_2 \tag{32}$$

$$\varphi_1^{\mathsf{T}}\varphi_1 \leq \tfrac{3}{2}\|\Omega_e\|^2 + 3a^2\|q_e\|^2$$
$$\varphi_2^{\mathsf{T}}\varphi_2 \leq c_3 + 4c_1\|\Omega\|^2 + c_4\|\Omega_e\|^2$$

where $c_3 = 4c_0 + 4J^+d^+ + 4\dot{\Omega}_d^+$y $c_4 = 4\Omega_d^+$. Then, with $b_0 = c_3 + 3a^2, b_1 = 4c_1, b_2 = \frac{3}{2} + c_4$, the norm of $\|\varphi\|^2$ is given by

$$\|\varphi\|^2 = b_0 + b_1\|\Omega\|^2 + b_2\|\Omega_e\|^2. \tag{33}$$

The bound of the nonlinearities and disturbances depends on the angular velocity of the vehicle. In order to express (33) only in terms of the error and desired angular velocity, an extended vector with the system state and the desired error velocity is defined

$$\tilde{x}_a = \begin{bmatrix} q_e \\ \Omega_e \\ R_e^{\mathsf{T}}\Omega_d \end{bmatrix} = \begin{bmatrix} x_a \\ R_e^{\mathsf{T}}\Omega_d \end{bmatrix}, \tag{34}$$

using (24) we can calculate the angular velocity of the vehicle $\Omega = \Omega_e + R_e^{\mathsf{T}}\Omega_d$, that can be expressed as:

$$\Omega = G_1\tilde{x}_a, \quad G_1 = \begin{bmatrix} 0_{3\times3} & I_{3\times3} & I_{3\times3} \end{bmatrix},$$

the norm of the angular velocity $\|\Omega\|^2$ can be expressed in terms of the extended error vector (34) as

$$\|\Omega\|^2 = \tilde{x}_a^{\mathsf{T}}G_1^{\mathsf{T}}G_1\tilde{x}_a = \tilde{x}_a^{\mathsf{T}}G_2\tilde{x}_a, \ \ G_2 = \begin{bmatrix} 0_{3\times3} & 0_{3\times3} & 0_{3\times3} \\ 0_{3\times3} & I_{3\times3} & I_{3\times3} \\ 0_{3\times3} & I_{3\times3} & I_{3\times3}, \end{bmatrix}$$

then the norm of $\|\varphi\|^2$ from (33) can be expressed by

$$\|\varphi\|^2 = b_0 + \tilde{x}_a^{\mathsf{T}}G\tilde{x}_a, \ \ G = \begin{bmatrix} 0_{3\times3} & 0_{3\times3} & 0_{3\times3} \\ 0_{3\times3} & (b1+b2)I_{3\times3} & b_1I_{3\times3} \\ 0_{3\times3} & b_1I_{3\times3} & b_1I_{3\times3} \end{bmatrix}. \tag{35}$$

and the state x_a can be defined as

$$x_a = H\tilde{x}_a, \ \ H = \begin{bmatrix} I_{6\times6} & 0_{6\times3} \end{bmatrix} \tag{36}$$

4.4. Attitude Practical Stability

Consider the following control law

$$\tau = Kx_a \tag{37}$$

Theorem 1. *Suppose that*

1.- *The assumptions 1-3 are fulfilled*

2.- *For the system* (27) *with* (37)*, for some matrices* K *and* $P_a = P_a^{\mathsf{T}} > 0$ *(solution of the optimization problem* (46)*, when it exists), also some positive constants* $\alpha_a, \varepsilon_1, \varepsilon_2$ *that satisfy the inequality* $W_a(P_a, K, \alpha_a, \varepsilon_1, \varepsilon_2) < 0$ *where*

$$W_a = \begin{bmatrix} G_a & \varepsilon_1 G_{12} & P_a \\ \varepsilon_1 G_{12}^{\mathsf{T}} & (\varepsilon_1 b_1 - \varepsilon_2)I_{3\times3} & 0_{3\times6} \\ P_a & 0_{6\times3} & -\varepsilon_1 I_{6\times6} \end{bmatrix} \tag{38}$$

$$G_a = (A_a + B_aK + \tfrac{\alpha_a}{2}I_{6\times6})^{\mathsf{T}}P_a + P_a(A_a + B_aK + \tfrac{\alpha_a}{2}I_{6\times6}) + \varepsilon_1 G_{11},$$
$$G_{12} = \begin{bmatrix} 0_{3\times3} \\ b_1I_{3\times3} \end{bmatrix}, \ G_{11} = \begin{bmatrix} 0_{3\times3} & 0_{3\times3} \\ 0_{3\times3} & (b_1 + b_2)I_{3\times3} \end{bmatrix},$$

there exists an energy function $V_a(P_a, x_a)$ *that has a differential inequality defined as*

$$\dot{V}_a \leq -\alpha_a V_a(P_a, x_a) + \beta_a \tag{39}$$

where, β_a *is a positive constant.*

Then, there exists an invariant ellipsoid for the closed-loop system (27) *and* (37)*.*

Proof. In order to analyze the behavior for the system, the energy function is proposed:

$$V_a = x_a^{\mathsf{T}}P_a x_a, \tag{40}$$

Now, adding and subtracting $\varepsilon_1\|\varphi\|^2$ and αV in the derivative of (40) follows that

$$\begin{aligned}\dot{V}_a &= (A_a x_a + B_a K x_a + \varphi)^\mathsf{T} P_a x_a + \\ &\quad x_a^\mathsf{T} P_a (A_a x_a + B_a K x_a + \varphi) \pm \varepsilon_1 \|\varphi\|^2 \pm \alpha_a V_a\end{aligned} \tag{41}$$

Using (35) and (36) in (41) it follows

$$\begin{aligned}\dot{V}_a &\leq \begin{bmatrix} x_a \\ R_e^\mathsf{T}\Omega_d \\ \varphi \end{bmatrix}^\mathsf{T} \begin{bmatrix} G_3 & H^\mathsf{T} P_a \\ P_a H & -\varepsilon_1 I_{6\times 6} \end{bmatrix} \begin{bmatrix} x_a \\ R_e^\mathsf{T}\Omega_d \\ \varphi \end{bmatrix} \\ &\quad + \varepsilon_1 b_0 - \alpha_a V_a \pm \varepsilon_2 \|R_e^\mathsf{T}\Omega_d\|^2 \\ &\leq \begin{bmatrix} x_a \\ R_e^\mathsf{T}\Omega_d \\ \varphi \end{bmatrix}^\mathsf{T} \begin{bmatrix} G_a & \varepsilon_1 G_{12} & P_a \\ \varepsilon_1 G_{12}^\mathsf{T} & (\varepsilon_1 b_1 - \varepsilon_2) I_{3\times 3} & 0_{3\times 6} \\ P_a & 0_{6\times 3} & -\varepsilon_1 I_{6\times 6} \end{bmatrix} \begin{bmatrix} x \\ R_e^\mathsf{T}\Omega_d \\ \varphi \end{bmatrix} \\ &\quad + \varepsilon_1 b_0 + \varepsilon_2 \Omega_d^+ - \alpha_a V_a\end{aligned} \tag{42}$$

where $G_3 = H^\mathsf{T}((A_a + B_a K + \frac{\alpha_a}{2} I_{6\times 6})^\mathsf{T} P_a + P_a(A_a + B_a K + \frac{\alpha_a}{2} I_{6\times 6}))H + \varepsilon_1 G$, Then, the equation (41) can be expressed as

$$\dot{V}_a \leq \begin{bmatrix} \tilde{x}_a \\ \varphi \end{bmatrix}^\mathsf{T} W_a \begin{bmatrix} \tilde{x}_a \\ \varphi \end{bmatrix} - \alpha_a V_a + \beta_a \tag{43}$$

where $\beta_a = \varepsilon_1 b_0 + \varepsilon_2 \Omega_d^+$.

Assuring that the matrix $W_a \leq 0$, the following inequality is guaranteed

$$\dot{V}_a \leq -\alpha_a V_a + \beta_a \tag{44}$$

and assures that the stability region is defined by the ellipsoid given by

$$\mathcal{E}_a = \left\{ x_a \in \mathbb{R}^n |\ x_a^\mathsf{T} P_a x_a \leq \frac{\beta_a}{\alpha_a} \right\} \tag{45}$$

Now, the minimization of the stability region can be found using the following optimization problem

$$\begin{aligned} &\operatorname{tr}\left\{ \tfrac{\beta_a}{\alpha_a} P_a^{-1} \right\} \to \min_{\alpha_a, \beta_a, \varepsilon_1, \varepsilon_2, K, P_a} \\ &\quad \text{subject to the restrictions} \\ &\quad \alpha_a > 0,\ \varepsilon_1 > 0,\ \varepsilon_2 > 0, \\ &0 < P_a,\ W_a = W_a(K, P_a, \alpha_a, \varepsilon_1, \varepsilon_2) \leq 0 \end{aligned} \tag{46}$$

which can be solved by using the MATLAB toolboxes SeDuMi and YALMIP through the Interior Point Method [25].

□

5. Position Control Design

Now with an attitude control, we proceed to the design of the control law for the position dynamics, and how should be computed the virtual control in order to assure the tracking of the desired position.

5.1. Observer equations

A way of estimate the velocity of the vehicle is needed because only position measurement is available. Using a dirty derivative, although easy to implement, increases the noise present in the signals of position. In order to reduce the noise an observer is proposed to estimate the velocity of the vehicle.

A space state of the position is defined as

$$x_\xi = \begin{bmatrix} x_{\xi_1} \\ x_{\xi_2} \end{bmatrix} = \begin{bmatrix} \xi \\ \dot{\xi} \end{bmatrix} \tag{47}$$

with the position dynamics

$$\ddot{\xi} = \frac{1}{m}(u_o + f_d(t)), \quad u_o = -TR(\overline{q})e_z + mge_z \tag{48}$$

$\dot{x}_\xi$ and the output of the system are

$$\dot{x}_\xi = A_p x_\xi + B_p u_o + B_p f_d(t), \quad y = C x_\xi + \eta \tag{49}$$

where $\eta \in \mathbb{R}^3$ represents the noise present in the measurements,

$$A_p = \begin{bmatrix} 0_{3\times 3} & I_{3\times 3} \\ 0_{3\times 3} & 0_{3\times 3} \end{bmatrix},\ B_p = \begin{bmatrix} 0_{3\times 3} \\ \frac{1}{m} I_{3\times 3} \end{bmatrix},\ C = \begin{bmatrix} I_{3\times 3} & 0_{3\times 3} \end{bmatrix}$$

and the observer equation is given by

$$\dot{\hat{x}}_\xi = A_p \hat{x}_\xi + B_p u_o + L(y - C\hat{x}_\xi). \tag{50}$$

where $L \in \mathbb{R}^{6\times 3}$.

5.2. Position Error Equations

In order to analyze how the virtual control affects the position stability, let introduce this term in the position dynamics. From (1) adding and substracting the virtual control u_d defined in (12), and $T_d R(\overline{q})e_z$, the acceleration is given by

$$m\ddot{\xi} = u_d + f_d(t) + \zeta_\xi(T, T_d, \overline{q}, \overline{q}_d) + mge_z \tag{51}$$

where

$$\zeta_\xi(T, T_d, \overline{q}, \overline{q}_d) = (-T_e R(\overline{q}) + T_d R(\overline{q}_d)(I_{3\times 3} - R(\overline{q}_e)))e_z \tag{52}$$

Note that $\zeta_\xi(T, T_d, \overline{q}, \overline{q}_d) = 0$ if $T = T_d$ and $\overline{q} = \overline{q}_d$. This means that the term ζ_ξ can be seen as a disturbance produced by the difference of the desired and the actual input forces in the position dynamics. Since the desired attitude gives the direction of the input force vector, then the norm of ζ_ξ increases as the attitude error grows.

The desired position state is defined by

$$x_d = \begin{bmatrix} \xi_d \\ \dot{\xi}_d \end{bmatrix} \tag{53}$$

Now the error for the position and observer dynamics are defined as

$$\begin{aligned} \tilde{x}_e &= \hat{x}_\xi - x_d && \text{estimated position error} \\ \hat{x}_e &= \hat{x}_\xi - x_\xi && \text{observed position error} \\ x_e &= x_\xi - x_d && \text{real position error} \end{aligned} \tag{54}$$

Then, using (47), (54) and (51) the error dynamics is expressed as

$$\dot{x}_e = \begin{bmatrix} \dot{\xi} - \dot{\xi}_d \\ \frac{1}{m}(u_d + f_d(t) + mge_z + \zeta_\xi(T, T_d, \overline{q}, \overline{q}_d)) - \ddot{\xi}_d \end{bmatrix} \tag{55}$$

Given that the gravity, mass and desired acceleration are well known, in the virtual control can be compensated the gravitational force and the desired acceleration, as a result the virtual controller is given by

$$u_d = u_p - mge_z + m\ddot{\xi}_d \tag{56}$$

where u_p is the feedback of the system signals. With (56), we can define a state space for the error dynamics as

$$\dot{x}_e = A_p x_e + B_p u_p + B_p \zeta_p, \tag{57}$$

where $\zeta_p = [0_{1\times 3}, (f_d(t) + \zeta_\xi(T, T_d, \overline{q}, \overline{q}_d))^\mathsf{T}]^\mathsf{T}$.

Defining the observer feedback controller as

$$u_p = K_p \tilde{x}_e, \tag{58}$$

from (49), (50) and (54), the equation of the observer error is defined by

$$\dot{\hat{x}}_e = (A_p - LC)\hat{x}_e - B_p f_d(t) + L\eta. \tag{59}$$

also, using (54) it follows that $\tilde{x}_e = x_e + \hat{x}_e$, then from (55), the position error dynamics is expressed as

$$\dot{x}_e = (A_p + B_p K_p)x_e + B_p K_p \hat{x}_e + B_p \zeta_p \tag{60}$$

Defining an extended error for the position error variables that we seek to stabilize $x_p = [x_e^\mathsf{T}, \hat{x}_e^\mathsf{T}]^\mathsf{T}$, which time derivative is using (60) and (59)

$$\dot{x}_p = \tilde{A}x_p + \tilde{B}\tilde{\zeta}_p \tag{61}$$

where $\tilde{\zeta}_p^\mathsf{T} = [\zeta_\xi{}^\mathsf{T} \ f_d(t)^\mathsf{T} \ \eta^\mathsf{T}]^\mathsf{T}$, $\tilde{A} = \begin{bmatrix} A_p + B_p K_p & B_p K_p \\ 0_{6\times 6} & A_p - LC \end{bmatrix}$, $\tilde{B} = \begin{bmatrix} B_p & B_p & 0_{6\times 3} \\ 0_{6\times 3} & -B_p & L \end{bmatrix}$

5.3. Assumptions of the Position Dynamics

Assumption 4: The rotor dynamics are fast, meaning that the time delay between the instant that desired thrust (T_d) is commanded and the instant that the actuators actually give that force is considered small enough to be neglected, and it can be assumed that the desired thrust is equal to the system thrust $T_d = T$.

Assumption 5: Part of the disturbances in the acceleration error in (55) are caused by the attitude error represented in the term $\zeta_\xi(T_d, \overline{q}, \overline{q}_d)$. That means that the disturbances grows as the attitude error q_e increases. Assuming that this term has an upper bound implies that the attitude error vector q_e has an upper bound, that indicates that the attitude controller assures that the norm of the vectorial part of the error quaternion $\|q_e\| \leq q_e^+ < 1$, where q_e^+ is a positive constant.

Assumption 6: The thrusters of the vehicle have an upper limit in the generated force, then there exists a positive constant $T^+ > T$.

Assumption 7: The external forces in the position dynamics $f_d(t)$ has an upper bound, then, there exists a positive constant f_d^+ such that $\|f_d(t)\|^2 < f_d^+$.

Assumption 8: The position noise measurement has a bound, there exists a positive constant η^+ such that $\|\eta\|^2 < \eta^+$, where $\eta \in \mathbb{R}^3$ represents the noise present in the measurements.

The disturbance due to the attitude error can be bounded if the assumptions 4-6 are fulfilled as follows:

$$\zeta_\xi^\mathsf{T}\zeta_\xi = T_d^2 \left((I_{3\times 3} - R(\overline{q}_e))\right)e_z)^\mathsf{T} \left(I_{3\times 3} - R(\overline{q}_e)\right))e_z \leq 2{T^+}^2 {q_e^+}^2 \tag{62}$$

5.4. Practical Stability with Observer Feedback

Now we seek that the observer and position error converges to a small enough stable region around the origin.

Theorem 2. *Suppose that:*

1.- *The assumptions 4-7 are fulfilled.*

2.- *For the system* (59) *and* (60) *with* (58)*, for some matrices K_p, L and $P = P^\mathsf{T} > 0$, also some positive constants α, ε that satisfy the inequality $W_p(P, K_p, L, \alpha, \varepsilon) < 0$ where*

$$W_p = \begin{bmatrix} P\tilde{A} + \tilde{A}^\mathsf{T}P + \alpha P & P\tilde{B} \\ \tilde{B}^\mathsf{T}P & -\varepsilon I_{9\times 9} \end{bmatrix}, \tag{63}$$

there exists an energy function $V(P, x_p)$ with the following differential equation

$$\dot{V} \leq -\alpha V + \beta \tag{64}$$

where $\beta > 0$.

As a result, there exists a stability region around the origin of x_e and $\hat{x}_e$ defined by the ellipsoid

$$\mathcal{E} = \left\{ x_p \in \mathbb{R}^n | \ x_p^\mathsf{T} P x_p \leq \frac{\beta}{\alpha} \right\} \tag{65}$$

Proof. In order to analyze the system, a energy function is proposed

$$V_p = x_p^\mathsf{T} P x_p \tag{66}$$

which derivative, using (62), adding and subtracting αV and $\varepsilon\|\tilde{\zeta}_p\|^2$, using assumptions 7 and 8 for the bound of the disturbances and noise as $\varepsilon\|\tilde{\zeta}_p\|^2 \leq \varepsilon\|\zeta_\xi\|^2 + \varepsilon f_d^+ + \varepsilon\eta^+$, is equal to

$$\begin{aligned} \dot{V} &= x_p^\mathsf{T} P \dot{x}_p + \dot{x}_p^\mathsf{T} P x_p \pm \alpha V \pm \varepsilon\|\tilde{\zeta}_p\|^2 \\ &\leq \begin{bmatrix} x_p \\ \tilde{\zeta}_p \end{bmatrix}^\mathsf{T} W_p \begin{bmatrix} x_p \\ \tilde{\zeta}_p \end{bmatrix} - \alpha V + \beta \end{aligned} \tag{67}$$

where $\beta = \varepsilon {T^+}^2 {q_e^+}^2 + \varepsilon f_d^+ + \varepsilon n^+$. As long as it is assured that $W_p \leq 0$, there exists a stability region around the origin of x_e and $\hat{x}_e$ defined by the ellipsoid

$$\mathcal{E} = \left\{ x_p \in \mathbb{R}^n |\ x_p^\mathsf{T} P x_p \leq \frac{\beta}{\alpha} \right\} \tag{68}$$

and the solution to the optimization problem is

$$\begin{gathered} \operatorname{tr}\left\{ \tfrac{\beta}{\alpha} P^{-1} \right\} \rightarrow \min_{\alpha,\beta,\varepsilon,K_p,P_a} \\ \text{subject to the restrictions} \\ \alpha > 0,\ \varepsilon > 0, \\ 0 < P,\ W_p = W_p\left(K_p, P, \alpha, \varepsilon, \right) \leq 0 \end{gathered} \tag{69}$$

□

As was mentioned in Assumption 5, the disturbances term ζ_ξ in the position error dynamics depends on the attitude error q_e, meaning that if the attitude controller doesn't assure the tracking of the desired references computed from the virtual controller, the position error will increase. In this sense, the stability of the position dynamics depends on the attitude stability, ie as $q_e \rightarrow 0$ implies $\xi_e \rightarrow 0$.

Note that for the derivative of the control $\dot{u}_d(\dot{\tilde{x}}_e, \dddot{\xi}_d) = K_p \ddot{\tilde{x}}_e + m \dddot{\xi}_d = K_p(\ddot{\tilde{x}}_e - \ddot{x}_d) + m \dddot{\xi}_d$, the $\ddot{\tilde{x}}_e$ can be estimated using (50). Also the term $\dddot{\xi}_d$ is needed, which implies that the desired position trajectory needs to be at least 4 times differentiable.

6. Numerical Results

In order to demonstrate the performance of the controller a simulation study subject to a time-varying wind gust and noisy measurements was implemented. The vehicle accomplishes the tracking of a position trajectory while tracking a desired ψ_d angle.

6.1. Simulator

The simulation was carried out using Matlab ® Simulink ® 9.2. The solver used was Dorman-Price (ode8) with a fixed step of $0.001s$. The Fig. 4 shows how the signals were used to calculate the controllers and dynamics of the simulated system. In order to emulate a real scenario, a

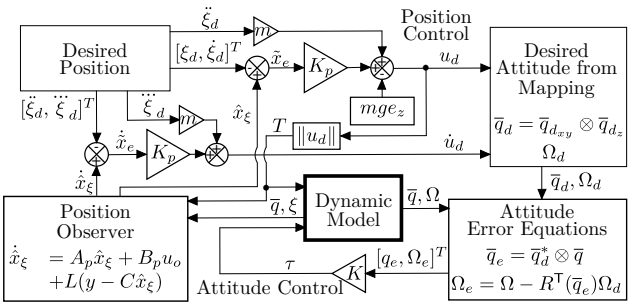

Figure 4: Block diagram of the control algorithm.

time-varying wind gust is simulated, where the wind velocity vector is $\sin^2(0.1\,t)\,[0.5403,\ 0.8415,\ 0]^\mathsf{T}$ m/s. Note that the magnitude of such a vector is $v(t) = \sin^2(0.1\,t)$ m/s. This wind gust generates state-dependent aerodynamical disturbances in the form of forces and moments that affect both position and orientation dynamics. The aerodynamic coefficients and the equations that describe these effects are [26]:

$$f_d = \frac{1}{2}\rho_a v_r^2\, S\, R\, W_d^\mathsf{T} \begin{bmatrix} c_L \\ c_Y \\ c_D \end{bmatrix}$$

$$\tau_d = \frac{1}{2}\rho_a v_r^2\, S \begin{bmatrix} b\, c_l \\ \bar{c}\, c_m \\ b\, c_n \end{bmatrix}$$

where the coefficients $\bar{c}$ and b are the chord and the span of a blade, respectively, c_D, c_Y, c_L, c_l, c_m and c_n are aerodynamical non-dimensional coefficients of drag, sideforce lift, rolling, pitching and yawing moments, respectively.

$$v_r = \sqrt{(v\sin(\alpha_0))^2 + (v\cos(\alpha_0) + v_i)^2}$$

and ρ_a is the air density, α_0 is the freestream angle of attack, v_r is the resultant velocity in the propeller slipstream, v_i is the induced velocity produced by the rotor, $v_i \approx \sqrt{\frac{T_m}{2\rho_a A_m}}$, and T_m is the thrust of the rotor and A_m is the area of the rotor disk. The orthogonal rotation matrix that relates the body fixed frame and the aerodynamic frame is

$$W_d = \begin{bmatrix} c_{\alpha_d} c_{\beta_d} & s_{\beta_d} & s_{\alpha_d} c_{\beta_d} \\ -c_{\alpha_d} s_{\beta_d} & c_{\beta_d} & -s_{\alpha_d} s_{\beta_d} \\ -s_{\alpha_d} & 0 & c_{\alpha_d} \end{bmatrix}$$

where $c_a = \cos(a)$ and $s_a = \sin(a)$, α_d is the angle of attack, $\alpha_d = \arctan\left(\frac{v\sin(\alpha_0)}{v\cos(\alpha_0)+v_i}\right)$ and β_d is the sideslip angle. The coefficients values used are $\rho_a = 1.19\,kg/m^3$, $\beta_d = 0$, $c_l = 0.15$, $c_m = 0.25$, $c_n = 0.8$, $c_L = 0$, $c_Y = 0.2$, $c_D = 0.1$, $S = 0.5\,m^2$, $b = 0.05\,m$, $\bar{c} = 0.02\,m$. $J = \operatorname{diag}(0.1241, 0.1241, 0.2483)\,kg\,m^2/rad$ and mass $m = 2kg$.

The initial conditions of the system are $q = [1, 0, 0, 0]^\mathsf{T}$, $\Omega = [0, 0, 0]^\mathsf{T}$ $\xi = [0, 0, -1]^\mathsf{T}$, $\dot{\xi} = [0, 0, 0]^\mathsf{T}$ and $\hat{x}_\xi = [0, 0, -1, 0, 0, 0]^\mathsf{T}$. Additionally, white noise is added to the position, attitude quaternion and angular velocity using the white noise block of Matlab ® Simulink, which generates normally distributed random numbers. Each block has different seed and the parameter noise power of 0.1. The values provided by those blocks are then multiplied by 0.0001 in order to obtain values between ± 0.003, which correspond approximately to a position error of $3mm$, attitude error of 0.4 degrees and angular velocity error of 0.003 rad/s. It is important to point out that a motion capture system Optitrack produces position error less than $0.3mm$ and rotational error less than 0.05 degrees [27].

The control parameters are given by:

$$K = [\text{diag}(10, 10, 10), \text{diag}(10, 10, 10)],$$
$$K_p = [-\text{diag}(40, 40, 40), -\text{diag}(80, 80, 80)],$$
$$L = [I; 100I]$$

The solution of LMIs from the optimization problem in the attitude dynamics is expressed as: $\lambda(P_a)_i \in \{0.017587, 0.45995\}$, $\varepsilon_1 = 0.0041433$, $\varepsilon_2 = 156.0903$ and $\alpha_a = 0.002973$; and for the position controller: $\lambda(P)_i \in \{0.0014673, 0.74522\}$, $\varepsilon = 2.8245$, $\alpha = 1.012$.

6.2. Task

The smooth desired trajectory, assuring small initial errors for position and attitude, is given by

$$\xi_d = \begin{bmatrix} \dfrac{r\left(\tanh\left(\delta t - 4\right) + 1\right)}{2} \cos\left(ft\right) \\ \dfrac{r\left(\tanh\left(\delta t - 4\right) + 1\right)}{2} \sin\left(ft\right) \\ -z_d \end{bmatrix} \tag{70}$$

The function tanh is used to slowly increase the radius of the circle from zero to a desired value r, where its increment depends on δ. This assures small initial errors provided that the initial position of vehicle is in the center of the circle. The trajectory parameters used were $\delta = 2$, $r = 1$, $f = 2$ and $z_d = 1$, with $\dot{\psi} = -2$ for the desired attitude. The desired trajectory is smooth enough to guarantee existence of $\dddot{\xi}_d$, which is a requirement for the solution of underactuation.

In order to calculate the desired trajectories for the attitude controller, the time derivative of the virtual position controller, u_d, is required. By using (50), it is computed as

$$\dot{u}_d = -K_p \dot{\tilde{x}}_e + m\dddot{\xi}_d = -K_p(\dot{\hat{x}}_\xi - \dot{x}_d) + m\dddot{\xi}_d$$

Note also that the term $\dddot{\xi}_d$ is needed to compute the desired angular velocity in (21). Thus, $\dddot{\xi}_d$ has to be continuous, which implies that the desired position trajectory needs to be at least 4 times differentiable.

6.3. Results

The tracking performance of the system is shown in Fig. 5. In Fig. 6, the 3D trajectory demonstrates how the vehicle begins in the center of the circle and increases the radius of the tracked circle until it reaches the target radius of 1. The system follows the desired trajectory with small errors, as can be appreciated in Fig. 7. The position controller is shown in Fig. 8. As seen from this figure, the element u_{d_3} reminds always negative, assuring that there is always a desired attitude at any given time. Fig. 9 shows the successful tracking of the desired attitude, computed from the position controller. However, the noise present in the position control results in a noisy

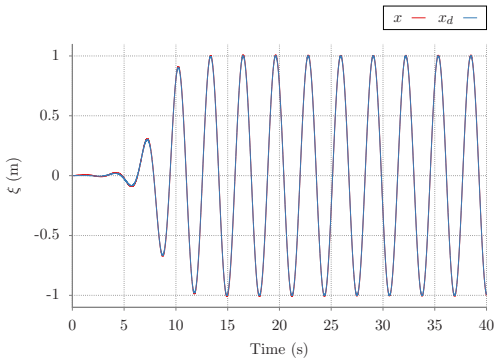

(a)

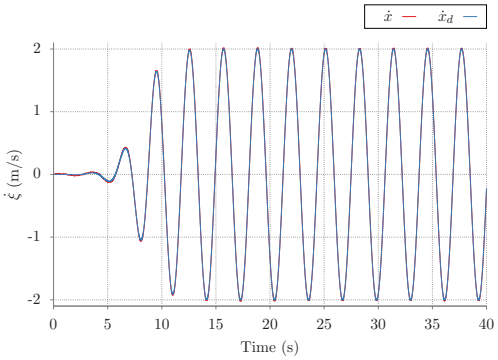

(b)

Figure 5: Position and velocity signals in the numerical results.

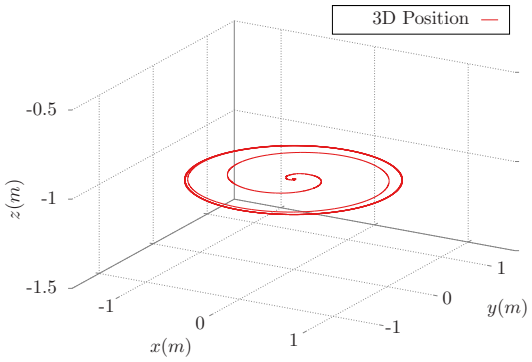

Figure 6: 3D position of the vehicle in the numerical results.

desired attitude trajectory, specially for the desired angular velocity. Even with this noise, the attitude is tracked with small errors, see Fig. 10, and consequently ensures position tracking at the same time. The attitude controller signals are presented in Fig. 11, which has a strong component of noise due to the noise present in the measured and desired signals. Finally, Fig. 12 shows the moment and force aerodynamical disturbances respectively that affect the vehicle.

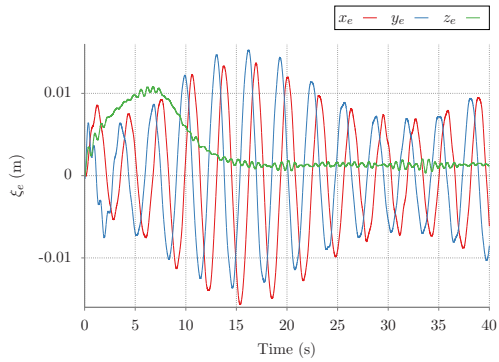

Figure 7: Position error in the numerical results.

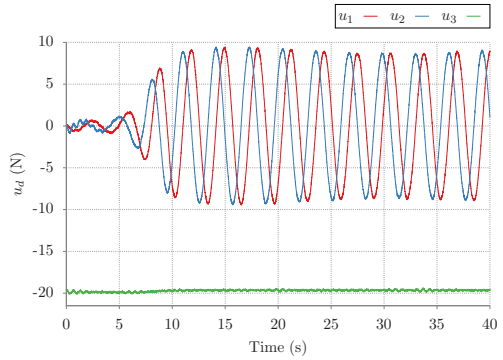

Figure 8: Position control signals in the numerical results.

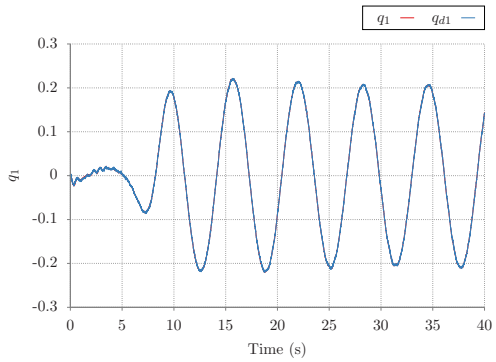

(a)

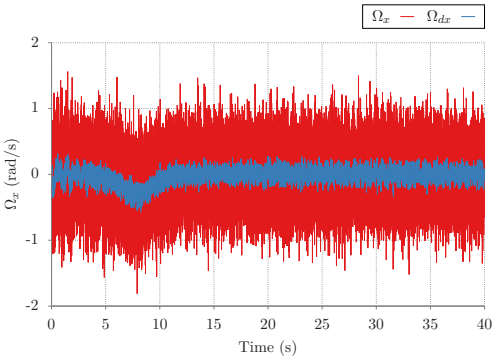

(b)

Figure 9: Attitude signals in the numerical results.

7. Experimental Results

The excellent performance of the control strategy is demonstrated when the aerial vehicle executes a similar trajectory to the one used in the numerical results, (70), a circle trajectory while tracking a desired angle ψ_d, using the equations (18) and (21). The platform used is an AR Drone 2.0 Edition of Parrot shown in Fig. 13. The platform uses a board with an ARM Cortex A8 1GHz processor with 1GB of RAM and the control algorithm is programmed in C++ code using Codeblocks 13 in a Linux Ubuntu 14.04 environment. The embedded system update the IMU measurements at $200Hz$ $(5ms)$, as well as control outputs to the rotors, interruptions, data fusion and communication to the ground station. The measurements of the position of the vehicle is performed using an Optitrack system with 24 cameras, that send information to the vehicle up to $100Hz$ $(10ms)$. The communication to the ground station allows to monitor the system measurements and change parameters in the controller and desired position, while all the data is recorded on board.

The parameters of the desired trajectory (70) are $\delta = 0.7$, $r = 1$, $f = 2$, $z_d = 1.5$ and $\dot{\psi}_d$ with initial condition $\psi_d(t_0) = 0$.

The control parameters used were:

$$K = [\text{diag}(4,4,4), \text{diag}(0.4,0.4,0.3)],$$
$$K_p = [\text{diag}(0.5,0.5,0.7), \text{diag}(0.4,0.4,0.5)],$$
$$L = [20I; 100I]$$

Using an approximation of the inertia matrix

$$J = \text{diag}(0.002237568, 0.002985236, 0.00480374)$$

and mass $m = 0.43kg$ for the optimization problem, the solution of the LMIs are for the attitude dynamics : $\lambda(P_a)_i \in \{7.5990e-05, 4.4614e-01\}$, $\varepsilon_1 = 0.055195$, $\varepsilon_2 = 2.0784$ and $\alpha_a = 0.00208$; and for the position controller: $\lambda(P)_i \in \{1.6117e-04, 3.2167e+00\}$, $\varepsilon = 1.8468$, $\alpha = 2.99$.

The result of the tracking of the desired position trajectory are shown in Fig. 14. The comparison of the measured and desired position is shown in Fig. 14(a), also, the comparison of the observed and desired velocity is displayed in Fig. 14(b), where it can be easily seen the outstanding tracking of the desired trajectory. Usually, given the underactuation of the quadrotor, the tracking of a circle seams that is out of phase [20], which in this case is not appreciable. It is better seen in Fig. 15 the error $\tilde{x}_e$, which magnitude is never greater than $20cm$ of the tracking of a $2m$ diameter circle.

In Fig. 16 the comparative of the two different forms to estimate the velocity of the vehicle is presented, one is a

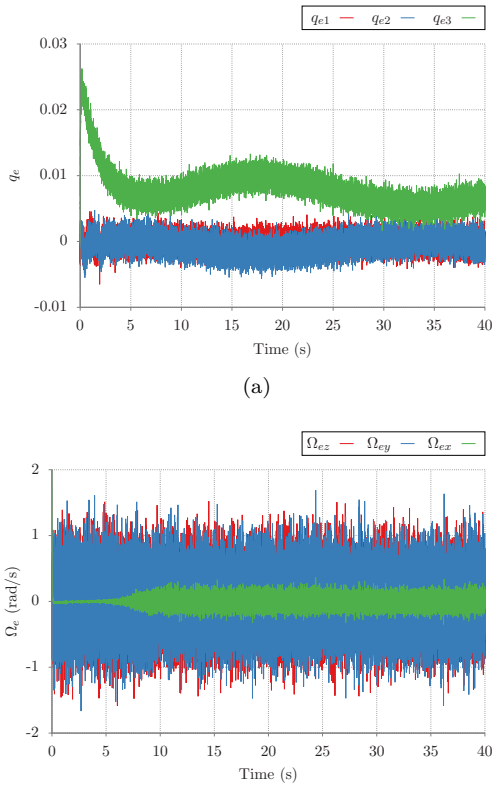

Figure 10: Attitude error signals in the numerical results.

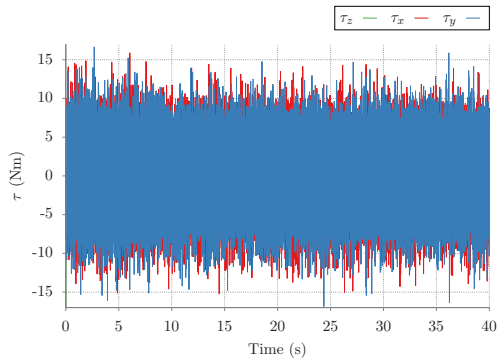

Figure 11: Orientation control signals in the numerical results.

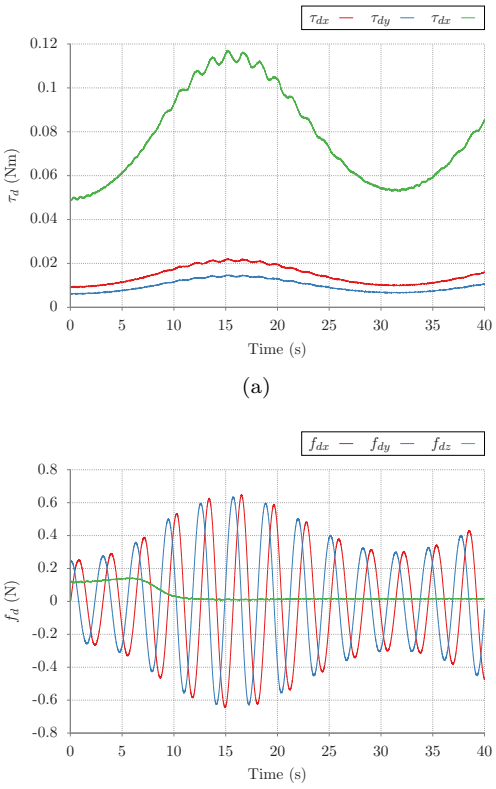

Figure 12: Torque and force disturbances in the numerical results.

Figure 13: Platform used for the experimental validation: Parrot AR Drone 2.0.

dirty derivative and the other one is using the observer. It is perceptible that the dirty derivative amplifies the noise present in the position measurements, while the observer estimate a more regular signal. This is important given that the desired attitude is computed using the error signals of position and velocity. Using more regular signals of the position and velocity signify more uniform desired trajectories for the orientation, making it easier for the attitude controller to perform the tracking, implying a better behavior in the position.

The virtual controller presented in Fig. 17, is used to estimate the desired quaternion. Given that the virtual controller contains noise, the desired quaternion and angular velocity also contains noise. The signals of the real quaternion components q_1, q_3 and the desired q_{1d}, q_{3d} (estimated from the virtual controller) are shown in Fig. 18. The main rotation is in the z axis, as can be seen in Fig. 18(b), the rotation about this axis has the same frequency as the circle, meaning that when the quadrotor finish a circle, a full 360º rotation is also completed. Even with noise present in the desired quaternion, the tracking has good performance, with small error in the attitude, as can be seen in the error quaternion vector from Fig. 19. The same applies to the angular velocity, shown in Figs. 20 and 21. Because the derivative of the desired rotation is $\dot{\psi} = 2$, the desired angular velocity Ω_{dz} has

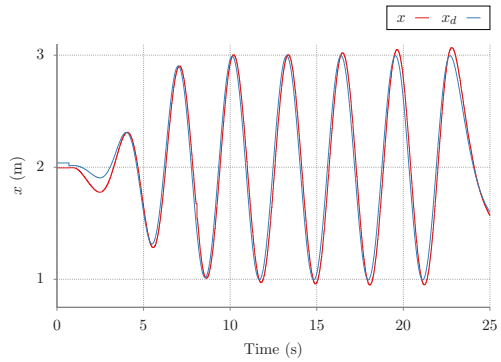

(a)

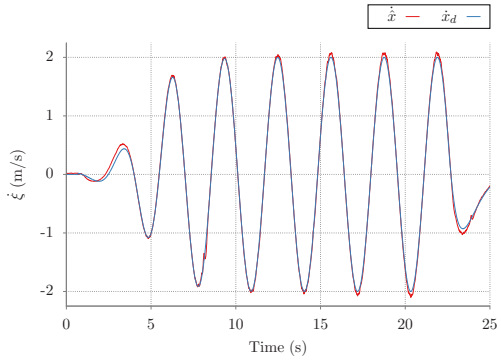

(b)

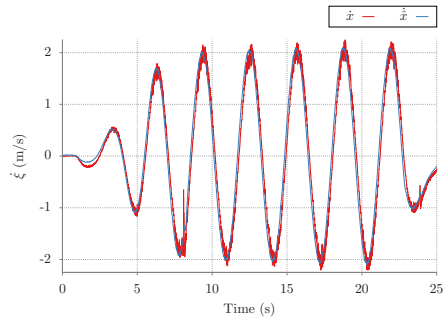

(c)

Figure 14: Position and observer signals in the experimental validation.

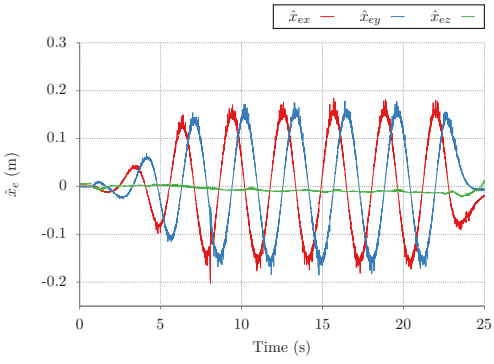

Figure 15: Observer error in the experimental validation.

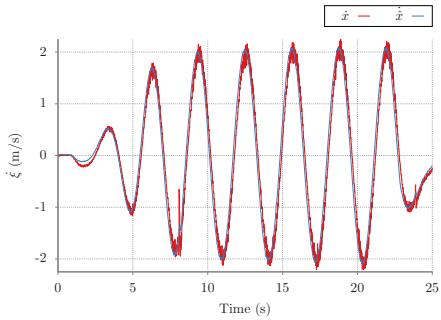

Figure 16: Comparison between dirty derivative and observer for the velocity estimation in the experimental validation.

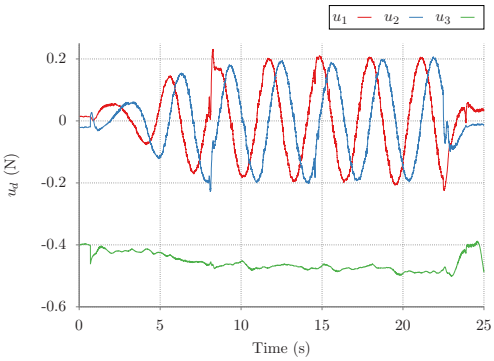

Figure 17: Virtual control signals during the experiment.

almost the same value plus some terms that come from the virtual controller as (21). The performance of the attitude controller is presented in Fig. 22. Fig. 23 shows the tracking in 3D space, where can be seen that as the diameter of the circle increases, the altitude error increments as well due to the increment of the inclination of the vehicle. Finally, Fig. 24 exhibits how the vehicle has to tilt in order to follow the desired trajectory, almost like looking to the center of the circle as following the desired rotation about the z axis. This trajectories has frequencies greater than usually used in quadrotors [18, 5, 28], also, for more aggressive trajectories the Euler angles may present singularities that jeopardize the integrity of the vehicle. The video of the experiments can be seen in `https://www.youtube.com/watch?v=1ZWpgedxMos`.

7.1. Implementation considerations

The design of the control is done without considering the latencies present in the vehicle, it is only assumed that the sampling rate is fast enough to be considered continuous. The vehicle has a sampling rate of $5ms$ for the attitude signals, which is small enough to have a response considered continuous. However solution of the optimization problem could lead to high gains that would induce higher frequencies than the maximum frequency response of the system leading to instability.

Also, a more aggressive trajectory in position implies a more aggressive trajectory in orientation, then, the invariant set for the attitude system could grow, leading to a

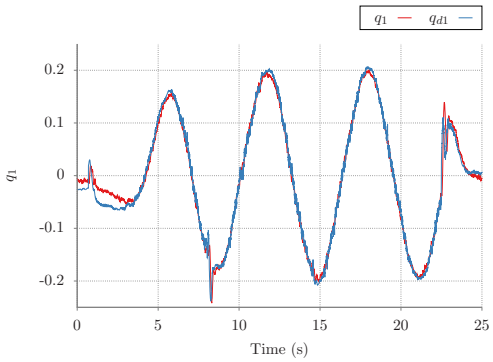

(a)

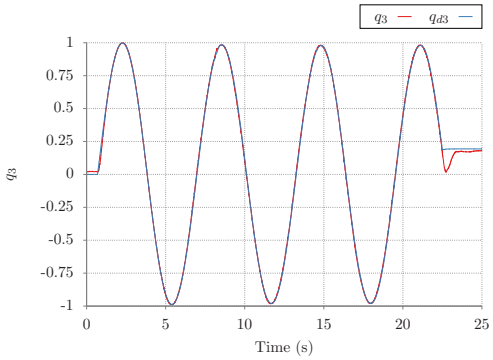

(b)

Figure 18: Attitude in the experiments.

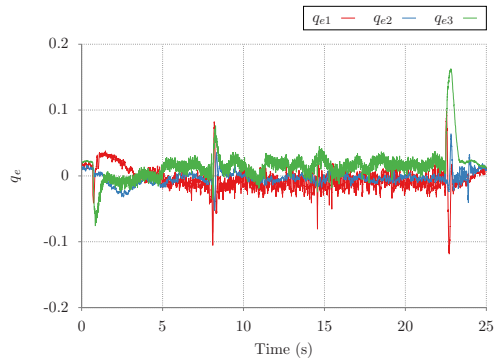

Figure 19: Attitude error in the experiments.

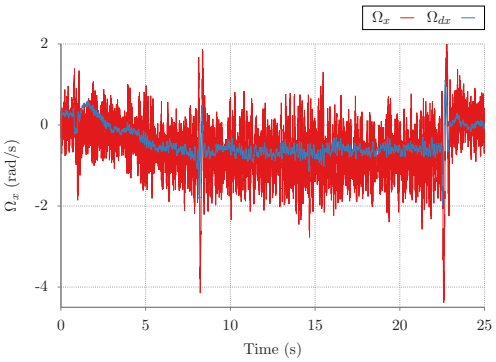

(a)

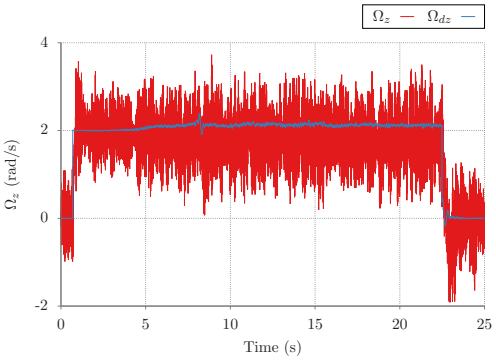

(b)

Figure 20: Angular velocity in the experiments.

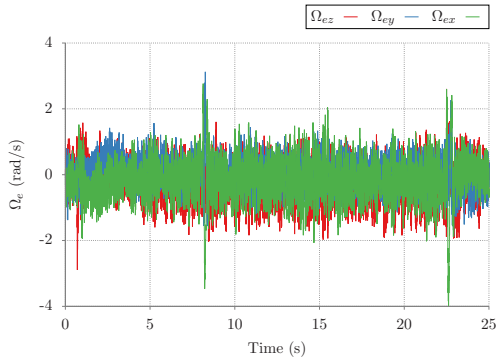

Figure 21: Angular velocity error in the experiments.

increase in the disturbance in position due to orientation error and therefore a greater error in position.

Given the small errors requirement for the small error initial condition, the vehicle needs to start near from the desired trajectory, or even in the desired trajectory. If the vehicle needs to reach a specific point, the desired path has to be designed in order that gently leads from the starting point(where the vehicle begins) to the end point(the desired position).

8. Conclusions

A continuous position control for a quadrotor using observer feedback was proposed. The ellipsoid method forced the error to a small enough region around the origin, which allowed the system to track the desired position, even for highly aggressive maneuvers. The solution of underactuation provided the attitude desired references, needed by the attitude controller for the purpose of tracking the position trajectory, through a unit quaternion in order to avoid the singularities. The only restriction on the proposed scheme is that the desired force never points downwards, which implies that there is no error in the x and y directions and the desired point in z is far beneath the ve-

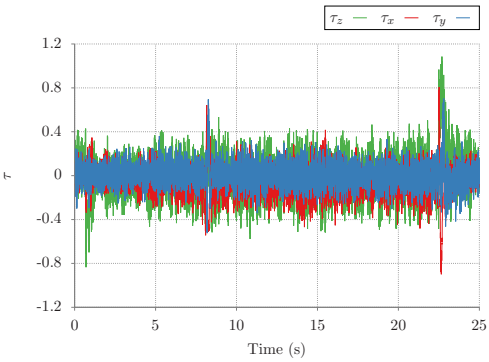

Figure 22: Attitude control signals during the experiment.

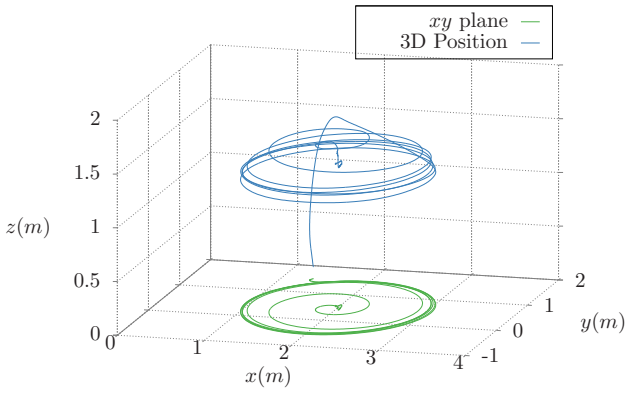

Figure 23: 3D view of position of the vehicle during the experiment.

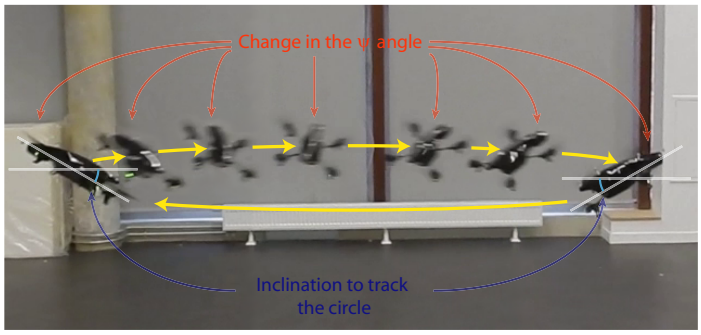

Figure 24: Different frames of the vehicle while performing the circle tracking and rotation about the z axis.

hicle, a highly improbable scenario. Finally, the proposed approach allows the tracking in 4 Dof, in this case the 3 Dof of position and the yaw angle.

Acknowledgment

Authors acknowledge partial support from Conacyt-Mexico under Research Grants 264513, 133344 and 133546. This work has been sponsored by the French government research program "Investissements d'avenir" through the Robotex Equipment of Excellence (ANR-10-EQPX-44).

[1] F. Oliva-Palomo, A. Muñoz-Vázquez, A. Sánchez-Orta, V. Parra-Vega, C. Izaguirre-Espinosa, P. Castillo, A fractional nonlinear pi-structure control for robust attitude tracking of quadrotors, IEEE Transactions on Aerospace and Electronic Systems doi:10.1109/TAES.2019.2893817.

[2] C. Izaguirre-Espinosa, A. J. Muñoz-Vázquez, A. Sánchez-Orta, V. Parra-Vega, P. Castillo, Attitude control of quadrotors based on fractional sliding modes: theory and experiments, IET Control Theory & Applications 10 (7) (2016) 825–832.

[3] S. Bouabdallah, R. Siegwart, Full control of a quadrotor, in: 2007 IEEE/RSJ International Conference on Intelligent Robots and Systems, 2007, pp. 153–158.

[4] J. Ferrin, R. Leishman, R. Beard, T. McLain, Differential flatness based control of a rotorcraft for aggressive maneuvers, in: 2011 IEEE/RSJ International Conference on Intelligent Robots and Systems, 2011, pp. 2688–2693.

[5] D. Cabecinhas, R. Cunha, C. Silvestre, A globally stabilizing path following controller for rotorcraft with wind disturbance rejection, IEEE Transactions on Control Systems Technology 23 (2) (2015) 708–714.

[6] D. Mellinger, N. Michael, V. Kumar, Trajectory generation and control for precise aggressive maneuvers with quadrotors, International Journal of Robotics Research 31 (5) (2012) 664–674.

[7] X. Shao, J. Liu, H. Wang, Robust back-stepping output feedback trajectory tracking for quadrotors via extended state observer and sigmoid tracking differentiator, Mechanical Systems and Signal Processing 104 (2018) 631–647.

[8] Z. Cai, J. Lou, J. Zhao, K. Wu, N. Liu, Y. X. Wang, Quadrotor trajectory tracking and obstacle avoidance by chaotic grey wolf optimization-based active disturbance rejection control, Mechanical Systems and Signal Processing 128 (2019) 636–654.

[9] L. Zhao, L. Dai, Y. Xia, P. Li, Attitude control for quadrotors subjected to wind disturbances via active disturbance rejection control and integral sliding mode control, Mechanical Systems and Signal Processing 129 (2019) 531–545.

[10] B. Wang, X. Yu, L. Mu, Y. Zhang, Disturbance observer-based adaptive fault-tolerant control for aquadrotor helicopter subject to parametric uncertainties andexternal disturbances, Mechanical Systems and Signal Processing 120 (2019) 727–743.

[11] Z. Cai, J. Lou, J. Zhao, K. Wu, N. Liu, Y. X. Wang, Quadrotor trajectory tracking and obstacle avoidance by chaotic grey wolf optimization-based active disturbance rejection control, Mechanical Systems and Signal Processing 128 (2019) 636–654.

[12] A. Tayebi, S. McGilvray, Attitude stabilization of a vtol quadrotor aircraft, IEEE Transactions on Control Systems Technology 14 (3) (2006) 562–571.

[13] L. Wang, J. Su, Switching control of attitude tracking on a quadrotor uav for large-angle rotational maneuvers, in: 2014 IEEE International Conference on Robotics and Automation (ICRA), 2014, pp. 2907–2912.

[14] A. A. El-Badawy, M. A. Bakr, Quadcopter aggressive maneuvers along singular configurations: An energy-quaternion based approach, Journal of Control Science and Engineering 2016.

[15] H. Hua, Y. Fang, X. Zhang, C. Qian, Auto-tuning nonlinear pid-type controller for rotorcraft-based aggressive transportation, Mechanical Systems and Signal Processing 145 (2020) 1–14.

[16] J.-J. Xiong, E.-H. Zheng, Position and attitude tracking control for a quadrotor uav, ISA Transactions 53 (3) (2014) 725 – 731.

[17] L. Zhao, L. Dai, Y. Xia, P. Li, Attitude control for quadrotors subjected to wind disturbances via active disturbance rejection control and integral sliding mode control, Mechanical Systems and Signal Processing 129 (2019) 531–545.

[18] A. Roberts, A. Tayebi, Adaptive position tracking of vtol uavs, IEEE Transactions on Robotics 27 (1) (2011) 129–142.

[19] X. Shao, N. Liu, Z. Wang, W. Zhang, W. Yang, Neuroadaptive integral robust control of visual quadrotor for tracking a moving object, Mechanical Systems and Signal Processing 136 (2020) 1–17.

[20] A. Sanchez, V. Parra-Vega, C. Tang, F. Oliva-Palomo,

C. Izaguirre-Espinosa, Continuous reactive-based position-attitude control of quadrotors, in: American Control Conference (ACC), 2012, 2012, pp. 4643–4648.
[21] A. Poznyak, A. Polyakov, V. Azhmyakov, Attractive Ellipsoids in Robust Control, Springer, 2014.
[22] X. Zhu, D. Li, Robust fault estimation for a 3-dof helicopter considering actuator saturation, Mechanical Systems and Signal Processing 155 (2021) 107624.
[23] J. B. Kuipers, Quaternions and rotation sequences: a primer with applications to orbits, aerospace and virtual reality, Princeton University Press, 1999.
[24] H. Alazki, A. Poznyak, Robust output stabilization for a class of nonlinear uncertain stochastic systems under multiplicative and additive noises: The attractive ellipsoid method, Journal of Industrial and Management Optimization 12 (1) (2016) 169–186.
[25] Y. Nesterov, A. Nemirovskii, Interior-Point Polynomial Algorithms in Convex Programming, SIAM Studies in Applied and Numerical Mathematics; vol. 13, 1994.
[26] H. Ramirez-Rodriguez, V. Parra-Vega, A. Sanchez-Orta, O. Garcia-Salazar, Robust backstepping control based on integral sliding modes for tracking of quadrotors, Journal of Intelligent & Robotic Systems 73 (2014) 51–66.
[27] Optitrack for robotics.
URL `https://optitrack.com/applications/robotics/`
[28] N. Cao, A. F. Lynch, Inner-outer loop control for quadrotor uavs with input and state constraints, IEEE Transactions on Control Systems Technology 24 (5) (2016) 1797–1804.